

# Ceria-Based Heterogeneous Catalyst for Organic Transformation

A Thesis

Submitted to

Indian Institute of Science Education and Research Pune in partial fulfilment of  
the requirements for the BS-MS Dual Degree Programme

By

**KOMAL KUMAR MEENA**

(20181020)



Indian Institute of Science Education and Research Dr. Homi Bhabha Road,  
Pashan, Pune 411008, INDIA.

April 2023

**Supervisor: Dr. Shubhangi B Umbarkar**

Scientist Catalysis Division,  
National Chemical Laboratory, Pune - 411008

All rights reserved

# Certificate

This is to certify that this dissertation entitled “**Ceria-Based Heterogeneous Catalyst for Organic Transformation**” towards the partial fulfilment of the BS-MS dual degree programme at the Indian Institute of Science Education and Research, Pune represents work carried out by **Komal Kumar Meena** at the National Chemical Laboratory, Pune under the supervision of **Dr. Shubhangi B Umbarkar**, Catalysis division, NCL Pune, during the academic year 2022-2023



Student's signature

Date: 10/04/2023



Supervisor's signature

Date: 10/04/2023

This thesis is dedicated to **my lovely family...**

# Declaration

I hereby declare that the matter embodied in the report entitled “**Ceria-Based Heterogeneous Catalyst for Organic Transformation**” is the result of the work carried out by me at the Catalysis Division, National Chemical Laboratory, Pune, under the supervision of **Dr. Shubhangi B Umbarkar** and the same has not been submitted elsewhere for any other degree.



Student's signature

Date: 10/04/2023

## Contents

Certificate.....	2
Declaration.....	4
Abbreviation .....	7
Symbols & Units .....	8
List of Figures .....	9
List of Schemes.....	10
List of Tables.....	10
Acknowledgements.....	11
Abstract.....	12
1. Introduction .....	13
1.1 Heterogeneous catalysis .....	15
1.2 Homogeneous catalysis.....	16
1.3 Principals of heterogeneous catalysis.....	17
1.4 Metal support interaction .....	18
1.5 Palladium (Pd) in Catalysis.....	19
2. Experiment details.....	21
2.1 Material.....	21
2.2 Synthesis of catalyst.....	21
2.2.1 Synthesis of ceria (CeO <sub>2</sub> ) & zirconia (ZrO <sub>2</sub> ) mixed oxides .....	21
2.2.2 Synthesis 1% palladium on ceria-zirconia oxides by impregnation .....	22
2.3 Characterizations of Catalyst .....	23
2.4 Catalytic activity for Mannich reaction .....	24
2.5 Catalytic activity for Suzuki coupling reaction .....	24
2.6 Analysis of reaction mixture.....	24
3. Results and Discussions .....	25
3.1 Characterizations of catalyst .....	25
3.1.1 Powder X-ray diffraction analysis .....	25
3.1.2 Brunauer-Emmett-Teller (BET) surface area analysis .....	26
3.1.3 Fourier Transform Infrared (FT-IR) Spectroscopic analysis .....	27
3.1.4 SEM analysis .....	28
3.1.5 TEM Analysis.....	29
3.1.6 X-ray photoelectron spectroscopy analysis .....	32
3.2 Catalytic activity for Mannich reaction .....	33
3.3 Catalytic activity for Suzuki coupling reaction .....	35
3.3.1 Base effect on Suzuki coupling reaction.....	36

3.3.2 Time profile study of Suzuki coupling reaction .....	36
3.3.3 Effect of catalyst composition on Suzuki coupling reaction.....	37
3.3.4 Effect of Temperature on Suzuki coupling reaction .....	37
3.3.5 Effect of Catalyst loading on Suzuki coupling reaction .....	37
4. Conclusion.....	38
References .....	38

## Abbreviation

BE	Binding energy
BET	Brunauer-Emmett-Teller
EDAX	Energy Dispersive X-ray Spectroscopy
FID	Flame Ionization Detector
TON	Turn over number
GC	Gas Chromatography
NMR	Nuclear magnetic resonance
P-XRD	Powder X-Ray Diffraction
XPS	X-ray Photoelectron Spectroscopy
TLC	Thin Layer Chromatography
TEM	Transmission Electron Microscopy
FTIR	Fourier-Transformed Infrared
GC-MS	Gas Chromatography-Mass Spectroscopy

## Symbols & Units

a.u.	Arbitrary Unit
mmol	millimole
atm	Atmospheric pressure
°C	Celsius (unit of temperature)
cm <sup>-1</sup>	Wavenumber
E <sub>a</sub>	Energy of activation
θ	Theta
λ	wavelength
%	Percentage
nm	Nanometer
Mol	Mole
s	Second
h	Hour
ν	Frequency
α	Alpha

# List of Figures

Figure 1.1 Energy profile diagram representing the catalytic reaction

Figure 1.2 Branches of catalytic science

Figure 1.3 Reaction mechanism and Energy distribution of a heterogeneously catalysed reaction

Figure 1.4 Contribution of various noble metals in research

Figure 1.5 Palladium catalysed different coupling reactions

Figure 3.1 Powder XRD patterns of (a)  $\text{CeO}_2$  – calcined at  $1000^\circ\text{C}$ ; (b)  $\text{Ce}_{0.75}\text{Zr}_{0.25}\text{O}_2$  – calcined at  $600^\circ\text{C}$ ; (c)  $\text{Ce}_{0.75}\text{Zr}_{0.25}\text{O}_2$  – calcined at  $1000^\circ\text{C}$ ; (d)  $1\%\text{Pd}/\text{Ce}_{0.75}\text{Zr}_{0.25}\text{O}_2$  – calcined at  $500^\circ\text{C}$

Figure 3.2 BET surface area analysis of (a)  $\text{Ce}_{0.75}\text{Zr}_{0.25}\text{O}_2$  calcined at  $600^\circ\text{C}$  (b)  $\text{Ce}_{0.75}\text{Zr}_{0.25}\text{O}_2$  calcined at  $1000^\circ\text{C}$

Figure 3.3 FTIR of  $1\%\text{Pd}/\text{Ce}_{0.75}\text{Zr}_{0.25}\text{O}_2$  catalyst

Figure 3.4 SEM images of (a)  $\text{Ce}_{0.75}\text{Zr}_{0.25}\text{O}_2$  calcined at  $1000^\circ\text{C}$ ; (b)  $1\%\text{Pd}/\text{Ce}_{0.75}\text{Zr}_{0.25}\text{O}_2$  calcined at  $500^\circ\text{C}$

Figure 3.5 TEM images of  $\text{Ce}_{0.75}\text{Zr}_{0.25}\text{O}_2$  calcined at  $600^\circ\text{C}$

Figure 3.6 TEM images of  $\text{Ce}_{0.75}\text{Zr}_{0.25}\text{O}_2$  calcined at  $1000^\circ\text{C}$

Figure 3.7 TEM images of  $1\%\text{Pd}/\text{Ce}_{0.75}\text{Zr}_{0.25}\text{O}_2$  calcined at  $500^\circ\text{C}$

Figure 3.8 a) Ce 3d, b) Zr 3d, c) Pd 3d, and d) O 1s XPS spectra

## List of Schemes

Scheme 3.1 Mannich reaction with reactant cyclohexanone, benzaldehyde and aniline

Scheme 3.2 possible mechanism for Mannich (three component) chemical reaction

Scheme 3.3 Suzuki coupling reaction of phenylboronic acid and bromobenzene

Scheme 3.4 Mechanism of Suzuki coupling reaction catalysed by Pd/Ceria-Zirconia

## List of Tables

Table 3.1 Surface characterization of supports

Table 3.2 Elemental analysis of catalysts by EDAX

Table 3.3 Effect of different bases on Suzuki coupling reaction

Table 3.4 Time profile study of Suzuki coupling reaction

Table 3.5 Effect of catalyst composition on Suzuki reaction

Table 3.6 Effect of temperature on Suzuki reaction

Table 3.7 Effect of catalyst loading on Suzuki reaction

# Acknowledgements

The writing of a project report is an independent and novice experience. It brings to test our patience, vigour & dedication. This project would not have been possible without the able guidance and help of faculties who contributed much to the creation and finishing of this research work and have been gracious in donating their valuable time.

My sincere gratitude and indebtedness to my supervisor **Dr. Shubhangi B Umbarkar** and TAC Member **Prof. V.G. Anand**, for igniting my passion for applied research in the field of inorganic chemistry (catalyst) and extending continuous support for my dissertation, which has helped me to clarify and deepen the content and presentation of my work. I am also grateful to the university and the department itself for everything that they have offered me during this course of time.

I would like to thank heart fully and sincerely to my mentor, Mrs. Mirabai Madhukar Kasabe who has helped me throughout the journey and for her constant guidance and inspiration throughout the project. She was always there to help me at any point. In addition, I want to express my heartfelt gratitude to Dr. Dhananjay Shahuraj Doke, Mr. Ankit Maharshi, Mr. Jayesh Shankar Mane, and Mr. Pavan Narayan Kalbande for their superb advice during my research project. Despite their hectic schedules over the course of my project work, I owe them a huge debt of gratitude for their assistance, wise counsel, insightful suggestions, and prompt assistance. Finally, I want to take a moment to thank my family and friends in the sincerest way possible. Without their generous love, unwavering patience, and unending support, my dissertation would not have been possible.

## Abstract

Cerium dioxide ( $\text{CeO}_2$ ) sometimes referred to as ceria, is a rare earth metal oxide that is extensively used in a large number of applications. It is a white or pale-yellow powder that conducts electricity well and cannot be dissolved in water. High thermal stability, exceptional chemical stability, a redox ( $\text{Ce}^{4+}/\text{Ce}^{3+}$ ) behavior and the capacity to serve as an oxygen storage material are just a few of ceria's special qualities. In addition to being employed in the creation of ceramic materials, fuel cells, and polishing agents, it is also used in other chemical reactions as catalysts, especially those involving oxidation and reduction. Ceria has attracted interest recently for its possible use in catalytic converters, renewable energy sources like solar cells, and hydrogen storage, among other things. It is clear that adding zirconia to ceria stabilizes it and enhances its activity, thermal stability, and oxygen storage capability. In this thesis different composition of ceria-zirconia oxide is synthesized by the hydrothermal method and palladium is loaded by the impregnation method. The properties present in the prepared mixed oxides were detected by using these techniques such as XRD, BET, FT-IR, XPS, SEM, EDAX, and TEM. The Mannich reaction was carried out with the finally prepared Catalyst  $\text{Ce}_{0.75}\text{Zr}_{0.35}\text{O}_2$  and  $1\% \text{Pd}/\text{Ce}_{0.75}\text{Zr}_{0.25}\text{O}_2$ . Suzuki reaction was carried out with Catalyst  $1\% \text{Pd}/\text{Ce}_{0.65}\text{Zr}_{0.25}\text{O}_2$ ,  $1\% \text{Pd}/\text{Ce}_{0.75}\text{Zr}_{0.25}\text{O}_2$  and  $1\% \text{Pd}/\text{Ce}_{0.85}\text{Zr}_{0.15}\text{O}_2$ . The analysis of these reactions was done by TLC, GC and GC-MS.

# 1. Introduction

The science of matter and how it changes at the atomic and molecular levels is how chemistry is typically defined. Hence, it focuses on atom collections like gases, molecules, crystals, and metals; it describes the composition and statistical characteristics of these structures as well as how they interact to generate the material, we use every day. The goal of this science is to comprehend the atom's unique characteristics and interactions [1]. Early human activities like using fire to prepare food, salt to preserve food, pigments in cave paintings, and dyes to make lovely clothes can all be linked to the use of chemistry [2]. Catalyst has been a very important role in all these and other chemical reactions. Although the term "catalysis" was first used by Swedish scientist Berzelius in 1835, it required many more years to define a catalyst. The prefix cata, which means down, and the lysein, which means to split or break, are the two Greek terms that gave rise to the word catalysis. "Catalysis is the acceleration of a slow chemical process by the presence of a foreign substance" that is called a catalyst, according to Ostwald's definition of the term in 1895 [3]. It is commonly known that catalysts decrease a reaction's activation energy, speeding up the progress of the reaction by adhering to the reactant molecule and associating with it but has no impact on the reaction's chemical equilibrium (Figure 1.1).

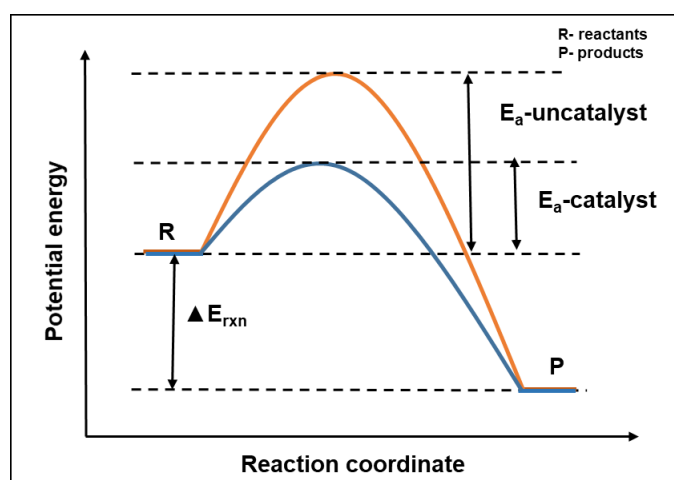


Figure 1.1 Energy profile diagram representing the catalytic reaction

A catalyst makes the procedure quicker without depleting it and aids in the conversion of several chemicals. As a result, it may change many reactant molecules simply by using catalytic quantities. Catalysis is one of the most important subfields in chemistry, and the most of compounds undergo at least one catalytic process throughout their production. Catalysis has considerably impacted the chemical industry and academics during the past century. In the chemical industry, catalysis-based processes account for 60% of current chemical compounds and 90% of dominant chemical processes [4].

Chemical engineering, inorganic chemistry, and organic chemistry are all involved in the multidisciplinary topic of catalysis. These are the three primary catalytic branches that led to the creation of an industrial process, as seen in Figure 1.2 [5]. Catalytic processes contribute to almost 90% of the production of all industrial chemicals. The catalytically produced intermediates have several uses in the chemical, petroleum, pharmaceutical, automotive, electronic materials, food, and energy sectors, among others [6].

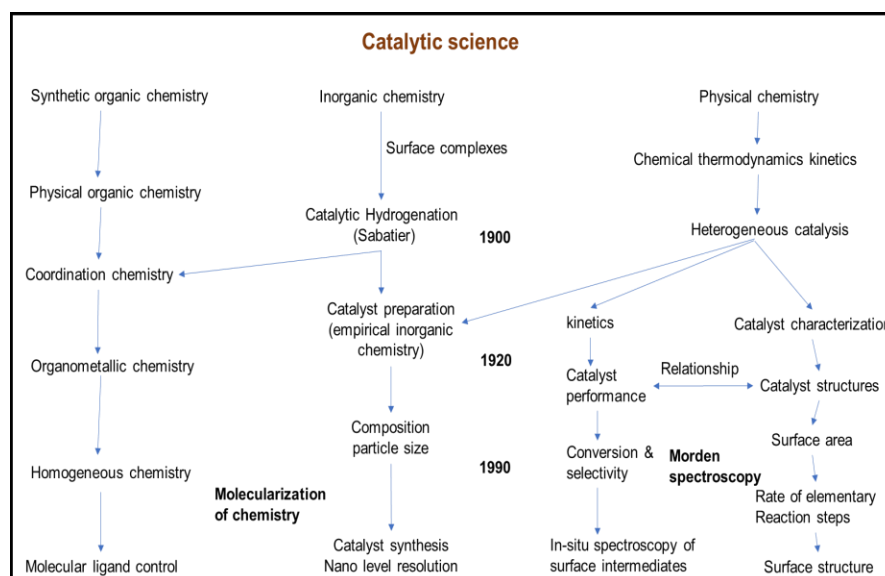


Figure 1.2 Branches of catalytic science

Catalysis had previously been mentioned as being used in the fermentation processes (the creation of wine and beer), sulphuric acid, cheese, soap, and others. In the early stages of its employment, the function of the catalyst remained unclear. The catalysis area has grown as a result of a comprehensive investigation into the causes

of the increase in reaction rate in the presence of a catalyst. As the precise function of the catalyst was discovered, its application for the manufacture of diverse compounds increased.

The inventor of the catalyst-based method for producing sulfuric acid (35%) was John Roebuck in 1746. In this procedure,  $\text{SO}_2$  is oxidised by  $\text{NO}_2$  in a large lead-lined chamber to produce sulfuric acid. Peregrine Phillips Jr. updated this procedure in 1831, employing a Pt catalyst to synthesize sulfuric acid with a high concentration. Alwin Mitach's study of the Haber-Bosch method of ammonia synthesis, which occurred in the previous century, was one of the most important catalytic turning points. Sooner or later, BASF Germany, which produces 20 tons of ammonia daily, received this technology. The ability of humans to boost food production is greatly impacted by the use of ammonia in fertilizers. Because of this, it is feasible to fulfill the need for food production even with a population that has increased from 1.6 billion in 1900 to 7.8 billion now [7].

Thus, many enterprises were formed for the production of chemicals, medicines, and fuels using catalysts in order to satisfy the demands of the expanding population at reasonable rates. From this, it can be seen that catalysis is crucial to both research activities and chemical processing. Different catalysts are constantly being developed to meet the demands of the economy and the environment. With the use of catalysis, a chemical reaction that causes pollution can be replaced with a more environmentally conscious approach [8].

According to the phase of the reactant and catalyst in the catalytic processes, there are generally two primary categories of catalysis.

- Heterogeneous catalysis
- Homogeneous catalysis

## 1.1 Heterogeneous catalysis

Heterogeneous catalysts have a catalyst presence during the reaction in a separate phase, often in solid form. The heterogeneous catalyst differs from the homogeneous catalyst in that it is simpler to separate from the products, which has allowed for ongoing chemical reactions. It has a high turnover number (TON) and a choice of a large variety of supports. In addition, heterogeneous catalysts are often more resistant to challenging working conditions than their homogeneous counterparts. Typically,

adsorption is a factor in the operation of heterogeneous catalysts. Adsorption of reactants from a reaction phase (liquid/gas) onto the solid catalytic surface is the principle of heterogeneous chemical transformation. The result is then desorption into the liquid or gas phase, followed by surface interaction between the adsorbed species. Another route to achieving the desired chemical reaction with less activation energy than in its absence is made possible by the presence of a catalyst in the process. It is obvious that a catalytic process will have far lower energy barriers than non-catalytic reactions, increasing the rate of reactions (Figure 1.3) [9].

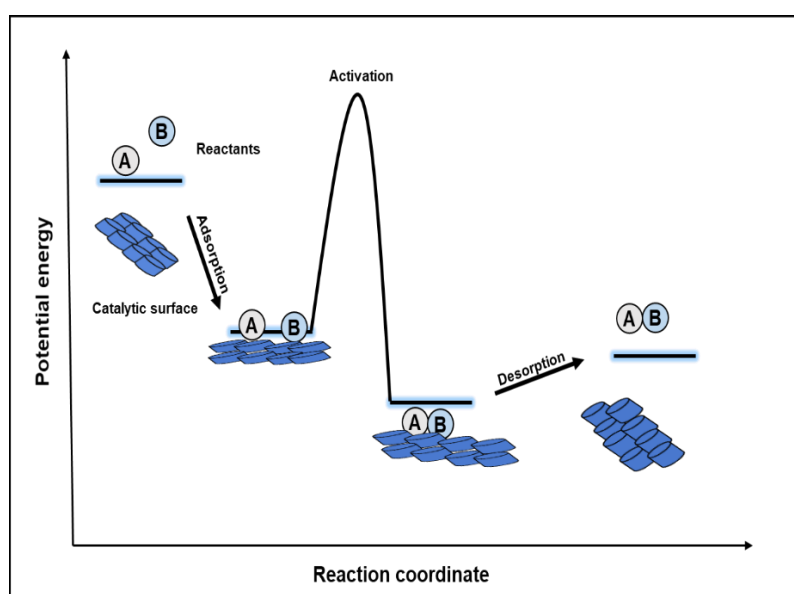


Figure 1.3 Reaction mechanism and Energy distribution of a heterogeneously catalysed reaction

## 1.2 Homogeneous catalysis

When a catalyst and reactants are in the same phase of a catalytic reaction, this is termed as homogeneous catalysis. Homogeneous catalysts are often coordination or solubility organometallic complexes that combine metal and ligands. These ligands offer metal complexes stability and increase the catalyst's reactivity with the target product. The high activity and selectivity (chemo-, region-, and enantio-) of the homogeneous catalysts are a result of the electrical interaction between the metal and ligands as well as the solubility of complexes. In 1938, Roelen produced the first

co-carbonyl-based homogeneous catalyst for the hydroformylation process. The Ziegler-Natta catalyst ( $\text{TiCl}_3$ ) was studied for the polymerization of ethylene and propylene in the 1950s, and this marked the beginning of precisely defined molecular complexes (coordination or organometallic) as catalytically active species. Wilkinson's achieved the most important  $\text{RhCl}(\text{PPh}_3)_3$  homogeneous complex finding for hydrogenation in 1965. Three triarylphosphine ligands in this combination serve to stabilize the central metal.

The organometallic complexes can be molecularly tuned with the assistance of the diversity of ligands. Currently, catalyst design is simpler thanks to advances in computer modelling, physical and chemical techniques, ligand synthesis, and large-scale industrial processes. Due to the discovery of asymmetric ligand systems, such as those used in the Monsanto method to produce L-Dopa, the area of enantiomeric catalysis has recently evolved [5]. The homogeneous catalyst category also includes biocatalysis. By utilising live (biological) systems or their components, biocatalysts accelerate chemical reactions. For instance, enzymes found in living organisms catalyse the chemical reaction of organic substances [10]. As biocatalysts frequently work with enzymes and microorganisms, they were formerly separated from homogeneous and heterogeneous catalysts and given their own classification. Nonetheless, it is classified as a homogeneous catalyst with a specific situation from a mechanistic perspective [11]. These biocatalysts are superior to other catalysts in large part because they demonstrated excellent chemo selectivity due to their activity for a particular type of functional group. The primary benefit of biocatalysts is that they are ecologically favorable since they are biodegradable. A Mild reaction state in biocatalysis reduces the unwanted side reactions, such as breakdown, racemization, isomerization, and rearrangement. Since catalysts are very stable and reusable when enzymes are attached on a substrate, continuous mode reactions in micro reactors are feasible [12].

### **1.3 Principals of heterogeneous catalysis**

The following steps are the most important part of heterogeneous catalysis.

- Reactant's adsorption on binding sites
- Desorption intermediates are formed or transformed during surface reactions, which may also entail surface diffusion processes.

- Desorption of products from binding sites.
- Intraparticle diffusion of the products through the catalyst pores.

Heterogeneous catalyst's catalytic activity is influenced by their varied chemical and physical characteristics. The center of a heterogeneous catalyst is comprised of active sites on the catalytic surface. The surface area of heterogeneous catalysts is often quite large (e.g., 10-1000 m<sup>2</sup>g<sup>-1</sup>). This surface area maximises the availability of active sites per unit volume, which is particularly desired. The porosity of the support also affects the catalytic characteristics of heterogeneous catalysis, apart from increase in the surface area. In heterogeneous catalysis, the particle size of the active component significantly impacts the catalytic activity; smaller the particle size greater is catalytic activity. Nanoparticles in addition to these also contribute to the large surface areas. Several active sites, including terraces, edges, kinks, and voids, may be found on the surfaces of these nanoparticles [13]. As the orientation of reactant molecules is determined by the crystal structure of the active metal, it plays a crucial role in defining the reaction's activity and selectivity. The active component may also possess redox properties that can be employed for catalytic reactions like oxidation in addition to these characteristics. The oxidation state of the metal in the active component as well as reduction potential of the catalyst has a significant impact on the activity of the catalyst in redox reactions. The activity and selectivity of a catalytic process are influenced by the catalyst's features, such as its acid/base properties. The metal ion often behaves as Lewis or Bronsted acids, and its counterpart demonstrates the fundamental feature(basic) [14].

## 1.4 Metal support interaction

Support is a key factor in heterogeneous catalysis. An inert support, such as silica or carbon, is an option. In the case of inert support, the activity of the active component (metal or metal oxide) does not be affected because of the support qualities. Yet, in the case of active supports, the metal-support interaction is altered significantly, impacting the activity of the active metal component [15a]. The electronic characteristics of the supported metal particles are significantly influenced by the nature of support mainly its acid-base properties and redox characteristics. The metal support interactions are governed principally by the free energies of the support

surface, active phase, and the interfacial free energy between the two components [15a]. Noble metals and transition metals have relatively high surface free energy [15b], hence tiny particles or crystallites frequently clump together to minimise surface area. As a result, support is required to stabilise these metal nanoparticles by fostering good metal-support interactions (MSI). These interactions between the metal and the support mostly have an impact on the physical characteristics and morphology of tiny particles. As a result, the catalytic activity is affected by the nature of the support or characteristics of the active metal particle. The electrical, geometrical, and bifunctional properties of metal, which are in charge of the stability, activity, and selectivity of the catalyst, are impacted by the strong metal support interaction [16]. The following variables affect the MSI in heterogeneous catalysis:

- Nature of the metal
- Nature of the support
- Method of catalyst preparation
- Precursors of metal and support in the synthesis

## **1.5 Palladium (Pd) in Catalysis**

Palladium is typically thought of as a pricey metal, yet it is 2-3 times less expensive than other noble metals (Pt, Au, and Rh). A helpful and well-known component of several catalytic systems is Pd. In certain instances, palladium-catalytic systems demonstrated excellent efficiency under moderate reaction conditions and permitted a broad variety of functional groups. Palladium catalysts enable unique transformations that are not achievable using conventional approaches. The application of palladium-based catalysts for the production of physiologically active and essential chemicals is a major area of scientific interest. The crucial and unique feature of palladium like the rapid adsorption of a massive quantity of hydrogen gas to create palladium hydride (PdH) makes it a highly effective catalytic element in chemical processes. On the surface of palladium, however, H<sub>2</sub> molecules dissociate with little to no activation energy barrier [17]. Moreover, palladium's electronegativity [18] primarily aids in the establishment of a polarised Pd-X bond as well as rather strong Pd-H and Pd-C bonds. It is simple to perform the crucial processes of oxidative addition, reductive elimination, and transmetallation due to palladium's variable oxidation states Pd(II), and Pd(0). According to statistics obtained from the internet,

Palladium has contributed to the highest number of publications (26.08%) in a variety of sectors since 1990 among the other noble metals (Figure 1.4).

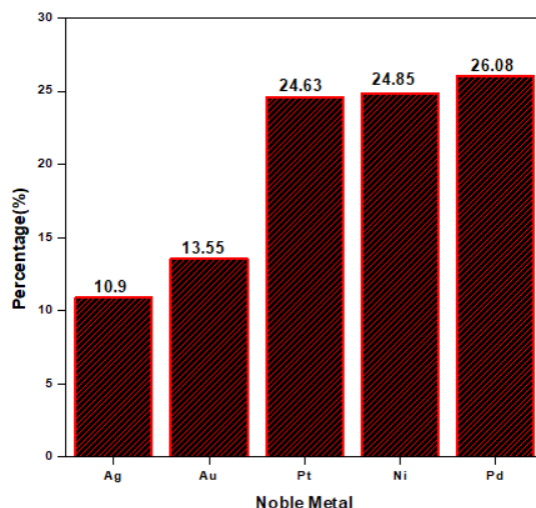


Figure 1.4 Contribution of various noble metals in research

Palladium is widely used in all areas of chemistry, including catalysis, organic synthesis, polymers, and materials. The simplicity of participation in chemical process transformations and the tolerance for the majority of functional groups are the fundamental reasons for this broad array. Palladium has been utilised extensively in a variety of sectors, including dehydrogenation [19], hydro-dehalogenation [20], hydrogenation [21], water gas shift [22], steam reforming [23], petroleum cracking [24], and oxidation reaction [25]. In most coupling processes, palladium is used as the core element in different complexes (Figure 1.5) [26].

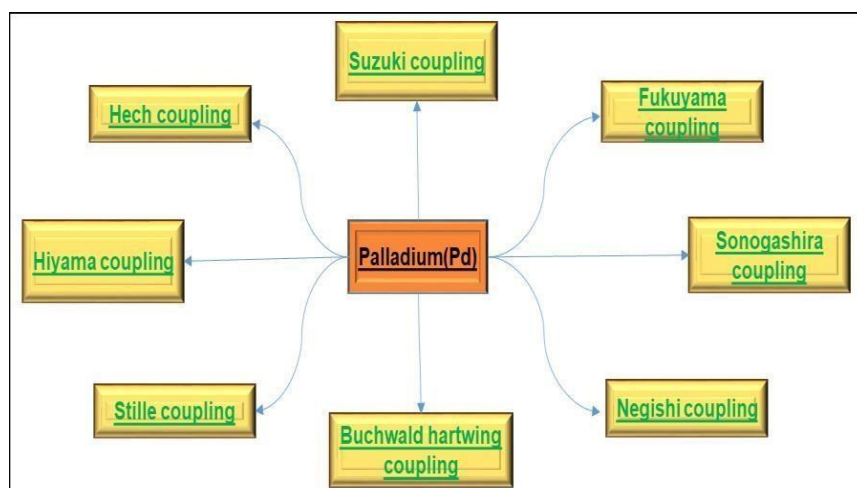


Figure 1.5 Palladium catalysed different coupling reactions

## 2. Experiment details

### 2.1 Material

All the reagents such as cerium nitrate hexahydrate, zirconyl chloride octahydrate were procured from Indian Rare Earths Ltd, ammonia solution, benzaldehyde, cyclohexanone, aniline, bromobenzene, phenylboronic acid, potassium, sodium and, calcium carbonate, sodium, calcium, potassium and barium hydroxide, sodium sulphate, isopropyl alcohol and all the solvents (ethyl acetate, pet ether, methanol, acetone) of AR grade were purchased from Thomas Baker, Lit, Himedia, chem labs, RFCL limited, LOBA Chemie, Sigma Aldrich Chemicals (India) and Unless otherwise noted, these materials were used without further purification.

### 2.2 Synthesis of catalyst

Catalyst is synthesized in many different ways. The catalytic activity depends on the method of synthesis. Here ceria and ceria's composition are synthesised by hydrothermal method and palladium (Pd) is loaded on the support by impregnation method.

#### 2.2.1 Synthesis of ceria (CeO<sub>2</sub>) & zirconia (ZrO<sub>2</sub>) mixed oxides

Cerium nitrate hexahydrate (Ce(NO<sub>3</sub>)<sub>3</sub>.6H<sub>2</sub>O) and zirconyl chloride octahydrate (ZrOCl<sub>2</sub>.8H<sub>2</sub>O) are precursors used for the synthesis of mixed oxides of ceria and zirconia.

The following procedure was followed to synthesize 25 gm Ce<sub>0.75</sub>Zr<sub>0.25</sub>O<sub>2</sub> composition.

A 10% solution of Ce(NO<sub>3</sub>)<sub>3</sub>.6H<sub>2</sub>O (47.65 gm) and ZrOCl<sub>2</sub>.8H<sub>2</sub>O (15.88 gm) was prepared by adding 630 ml distilled water and stirring well at room temperature. After mixing well for 30 min, ammonium hydroxide (5% NH<sub>4</sub>OH) was added drop by drop for precipitation till pH 9 was attained and the slurry was kept for 24h. Then the slurry was heated in a hydrothermal bomb at 120 °C for 40 min in a hot air oven. After cooling the slurry to room temperature, the solid was filtered and washed with water till neutral pH.

The solid sample was heated in a hot air oven at 100 °C for 24 h, and calcine at 500°C for 5h. Different compositions have been made by calcining in different temperatures, which areas follows:

$\text{CeO}_2$  (600°C) – calcined at 600°C

$\text{CeO}_2$  (1000°C) – calcined at 1000°C

$\text{Ce}_{0.75}\text{Zr}_{0.25}\text{O}_2$  (1000°C) – calcined at 1000°C

$\text{Ce}_{0.75}\text{Zr}_{0.25}\text{O}_2$  (500°C) – calcined at 500°C

$\text{Ce}_{0.85}\text{Zr}_{0.15}\text{O}_2$  (500°C) – calcined at 500°C

$\text{Ce}_{0.65}\text{Zr}_{0.35}\text{O}_2$  (500°C) – calcined at 500°C

### **2.2.2 Synthesis 1% palladium on ceria-zirconia oxides by impregnation**

Impregnation method- This method is used to load the metal in the prepared catalyst. In the catalytic support prepared by hydrothermal method, we loaded palladium in the following steps-

To load 1% palladium on 5gm  $\text{Ce}_{0.75}\text{Zr}_{0.25}\text{O}_2$  catalyst, we used palladium acetate ( $\text{Pd}(\text{OCOCH}_3)_2$ , 0.1082 gm). After grinding palladium acetate (0.1082 gm), it was thoroughly dissolved in 15 ml a 2:5 solvent system of acetone and methanol. A slurry of  $\text{Ce}_{0.75}\text{Zr}_{0.25}\text{O}_2$  (5gm) was prepared in 50ml distilled water. The palladium acetate solution was added dropwise with continuous stirring to the slurry of  $\text{Ce}_{0.75}\text{Zr}_{0.25}\text{O}_2$ . After adding, it was mixed continuously for 2 hours and after that, the remaining water was vaporized by heating on hot plate. The obtained sample was calcined at 250°C for 5h. Other compositions were prepared and calcined at different temperatures to understand the effect of calcining temperature. All compositions are like this

1%Pd/ $\text{Ce}_{0.65}\text{Zr}_{0.35}\text{O}_2$  (500°C) – calcined at 500°C

1%Pd/ $\text{Ce}_{0.75}\text{Zr}_{0.25}\text{O}_2$  (500°C) – calcined at 500°C

1%Pd/ $\text{Ce}_{0.85}\text{Zr}_{0.15}\text{O}_2$  (500°C) – calcined at 500°C

## 2.3 Characterizations of Catalyst

The properties of the synthesized catalysts and supports were investigated using these techniques.

**P-XRD-** Using a PAN analytical X-Pert Pro Dual Goniometer diffractometer, the produced catalysts were characterized by X-ray diffraction. The diffractometer made up of X'celerator solid state detector with  $\text{CuK}\alpha$  ( $\lambda=1.5406\text{\AA}$ , 40kV, 30mA) radiation and a Ni filter. The X-ray diffraction pattern of the sample was recorded in the range of  $2\theta = 20\text{-}80^\circ$  with a step size of  $0.02^\circ$  and a scan rate of  $4^\circ \text{ min}^{-1}$ .

**BET-** Using Autosorb Quanta Chrome equipment, the  $\text{N}_2$  sorption at  $-196^\circ\text{C}$  was used to calculate the catalyst's BET surface area. The material was evacuated at  $200^\circ\text{C}$  in a hoover prior to  $\text{N}_2$  adsorption. The Brunauer-Emmett-Teller equation was used to determine the specific surface area.

**FT-IR-** Thermo Nicolet Nexus 670 IR equipment with DTGS detector was used to capture the samples' Fourier Transform Infrared (FTIR) spectra. The samples were prepared using the KBr pellet method. Averaging over 100 scans, the spectra were acquired with a resolution of  $4 \text{ cm}^{-1}$  in the  $4000\text{-}300 \text{ cm}^{-1}$  region.

**SEM-** Using scanning electron microscopy (SEM) on an FEI Quanta 200 3D dual beam ESEM apparatus with thermionic emission tungsten filament in the 3 nm range at 30 kV, the morphology of the specimens was assessed.

**TEM-** Transmission electron microscopy was used to measure the particle size and d-spacing value, and the investigation was carried out using a Tecnai G2-20 FEI apparatus with a 300 kV accelerating voltage. The powder samples were ultrasonically mixed with isopropanol prior to examination, and two drops of isopropanol containing the solid were deposited on a carbon-coated copper grid.

**XPS-** A Thermo  $\text{K}\alpha$  spectrometer was utilised to conduct X-ray photoelectron spectroscopy (XPS) for the catalysts using micro-focused, monochromatic  $\text{AlK}\alpha$  radiation with an energy of 1486.6 eV. In a hoover chamber, the samples were degassed at 300K for 4 hours. The use of an electron flood cannon helped in the charge adjustment process. In order to calibrate binding energy (B.E.) measurements, the standard C 1s peak of contaminating carbon (284.6 eV) is used.

## 2.4 Catalytic activity for Mannich reaction

The catalytic activity for three component (Mannich) reaction was carried out in 50 ml round bottom flask at room temperature. The round bottom flask was charged with benzaldehyde (limiting reagent, 1gm), aniline (0.877gm), cyclohexanone (excess, 3.699gm), mole ratio (1:1:4) and 10 wt% catalyst  $\text{Ce}_{0.75}\text{Zr}_{0.25}\text{O}_2$  (with respect to limiting reagent).

## 2.5 Catalytic activity for Suzuki coupling reaction

The catalytic activity for the Suzuki cross-coupling (C-C) reaction was conducted in a 50 ml round bottom flask with different temperatures. The round bottom flask was charged with bromobenzene (1gm, 1mole), phenylboronic acid (0.931gm, 1.2mole), Sodium hydroxide (0.509gm, 2mole), 5wt % reduced catalyst 1%Pd/ $\text{Ce}_{0.75}\text{Zr}_{0.25}\text{O}_2$  (with respect to bromobenzene, 0.05gm), and 2ml water as solvent. The reaction flask was fitted with a reflux condenser.

CAUTION: Catalyst's reduction conducted by 10 minutes flow of hydrogen gas at room temperature under a fuming hood and with high safety concerns.

## 2.6 Analysis of reaction mixture

After the completion of the reaction, it was confirmed by TLC whether the product was formed or not, and after that the sample was centrifuged and the catalyst was separated from the reaction mixture. The liquid was filtered through a 0.22  $\mu\text{m}$  syringe filter to ensure free of catalyst. The reaction was monitored by GC using GC-SHIMADZU Corp. 80100 equipped with an HP-5 column (50 m length, 0.25 mm internal diameter, and 1  $\mu\text{m}$  film thickness) and flame ionization detector (FID). Yield of the reaction was calculated based on the GC-FID results. According to the GC response factors, the individual yields were determined.

## 3. Results and Discussions

### 3.1 Characterizations of catalyst

#### 3.1.1 Powder X-ray diffraction analysis

Figure 3.1 displays powder x-ray diffraction pattern of  $\text{CeO}_2$ ,  $\text{Ce}_{0.75}\text{Zr}_{0.25}\text{O}_2$  and 1%Pd/ $\text{Ce}_{0.75}\text{Zr}_{0.25}\text{O}_2$  calcined at different temperatures. The diffraction peaks at  $2\theta$  values of ceria ( $\text{CeO}_2$ ) were observed at 28.7, 33.2, 47.5, 56.3, 59.3, 69.8, 76.6, and 79.4°.

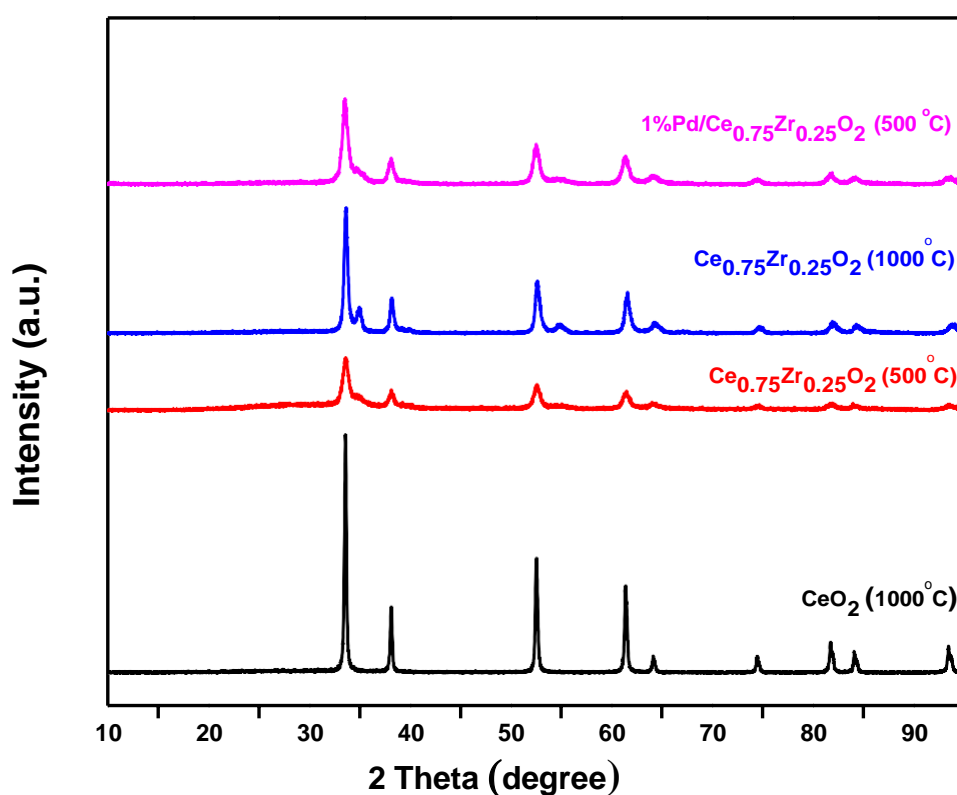


Figure 3.1 Powder XRD patterns of (a)  $\text{CeO}_2$  – calcined at 1000°C; (b)  $\text{Ce}_{0.75}\text{Zr}_{0.25}\text{O}_2$  – calcined at 600°C; (c)  $\text{Ce}_{0.75}\text{Zr}_{0.25}\text{O}_2$  – calcined at 1000°C; (d) 1%Pd/ $\text{Ce}_{0.75}\text{Zr}_{0.25}\text{O}_2$  – calcined at 500°C

The data from the Joint Committee on Powder Diffraction Standards (JCPDS) file no. 43-1002 from the International Centre for Diffraction Data support each of these

diffraction peaks. The  $Ce_{0.75}Zr_{0.25}O_2$  sample showed  $ZrO_2$  - corresponding diffraction peaks at  $2\theta$  values of 28.8, 31.8, 34.6, and 50.9. (JCPDS file no. 01-089-9066) [27]. In the sample of 1%Pd/ $Ce_{0.75}Zr_{0.25}O_2$ , palladium shows its  $2\theta$  intense peak at  $40^\circ$  but in our sample due to the low concentration of Pd (1%) it can't be seen in the XRD analysis. The broad diffraction peaks of Ceria-Zirconia reveal the small crystalline nature of the samples while increases calcine temperature intensity increases and peak width decreases observed due to an increase in the crystallinity.

### 3.1.2 Brunauer-Emmett-Teller (BET) surface area analysis

The textural properties of the prepared support ceria stabilised by 25% zirconia ( $Ce_{0.75}Zr_{0.25}O_2$ ) were investigated using the BET ( $N_2$  adsorption-desorption) surface analysis. The surface area measurements are given in table 3.1. The prepared support has shown a surface area of  $14.190\text{ m}^2/\text{g}$  at high temperature (Figure 3.2a) and a surface area of  $42.172\text{ m}^2/\text{g}$  at low temperature (Figure 3.2b). This implies that the surface area decreases as a result of the particle's propensity to aggregate at higher temperatures.

The detailed analysis showed (Figure 3.2) type IV isotherm with the H3 and H1 type of hysteresis confirming the mesoporous nature of the support. Support's mesoporous structure also was confirmed using data on pore size in the mesoporous region ( $3\text{nm} < \text{pore size} < 50\text{ nm}$ ) and the  $p/p_0$  isotherm range of 0.76-0.94. The prepared support has a specific surface area, pore diameter and pore volume.

Table 3.1 Surface characterization of supports

<b>Support type</b>	<b>Specific surface area (<math>\text{m}^2/\text{g}</math>)</b>	<b>Pore diameter (nm)</b>	<b>Pore volume (<math>\text{cm}^3/\text{g}</math>)</b>
$Ce_{0.75}Zr_{0.25}O_2$ ( $600^\circ\text{C}$ )	42.172	11.797	0.126
$Ce_{0.75}Zr_{0.25}O_2$ ( $1000^\circ\text{C}$ )	14.190	26.923	0.100

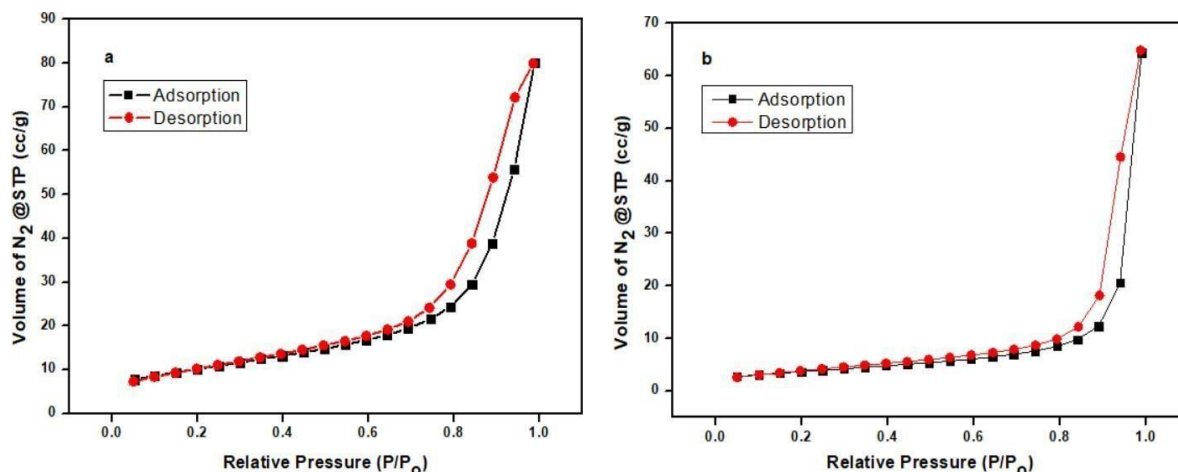


Figure 3.2 BET surface area analysis of (a)  $\text{Ce}_{0.75}\text{Zr}_{0.25}\text{O}_2$  calcined at  $600^\circ\text{C}$  (b)  $\text{Ce}_{0.75}\text{Zr}_{0.25}\text{O}_2$  calcined at  $1000^\circ\text{C}$

### 3.1.3 Fourier Transform Infrared (FT-IR) Spectroscopic analysis

Fourier-transform infrared spectroscopy is a technique used to quickly and definitively identify compounds by their symmetric & asymmetric stretching vibration. The FTIR spectra of the prepared catalysts are in the range of  $400\text{--}4000$  wavenumber ( $\text{cm}^{-1}$ ) shown in the Figure 3.3. Which identifies the chemical bonds as well as functional groups in the sample.

The absorption peak around  $1464\text{ cm}^{-1}$  is assigned to the bending vibration of C-H stretching. The intense band at  $500\text{ cm}^{-1}$  corresponds to the Ce-O stretching vibration [28]. The bands located at around  $741$ ,  $750$ , and  $1036\text{ cm}^{-1}$  have been attributed to the  $\text{CO}_2$  asymmetric stretching vibration,  $\text{CO}_3^{2-}$  bending vibration, and CO stretching vibration, respectively. Additionally, absorption peaks featured at the lower wavenumber of  $560\text{ cm}^{-1}$  are due to Zr-O vibrational stretch [29].

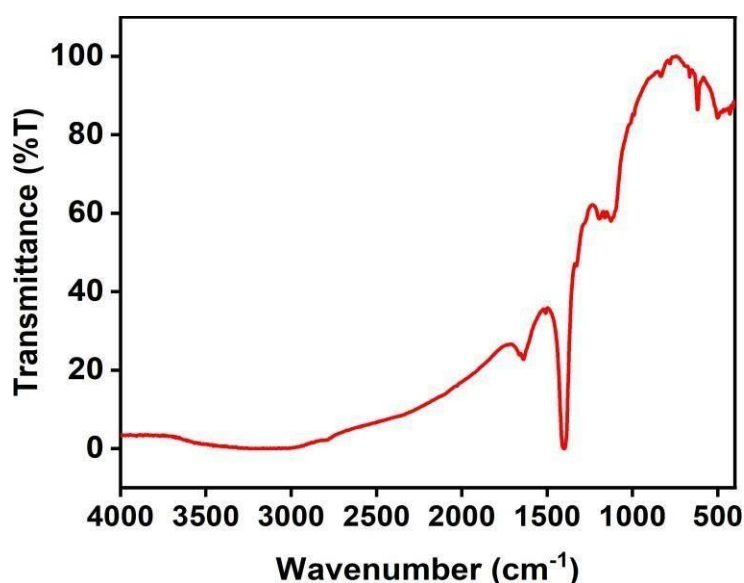


Figure 3.3 FTIR of 1%Pd/Ce<sub>0.75</sub>Zr<sub>0.25</sub>O<sub>2</sub> catalyst

From the FTIR analysis it was confirmed that our prepared catalyst is in complete oxide form and not in other hydroxide forms.

### 3.1.4 SEM analysis

To identify the morphology of catalysts, SEM investigation was carried out. Figure 2.5 displays the SEM images of the catalysts with and without Pd loading. The pictures of all catalysts were observed to have almost comparable morphology, despite it does not possess any particular morphology. It displayed a non-uniform particle size distribution, with some larger and some smaller (1-2 μm) particles.

The surface composition of catalysts was analysed using EDAX analysis. Table 3.2 displays the composition of the elements. Elemental analysis of the catalyst showed a similar amount of palladium actually added during the catalyst preparation. It implies that maximum amount of loaded palladium is available on the surface for reaction and maximum palladium is available to convert the reactant to product.

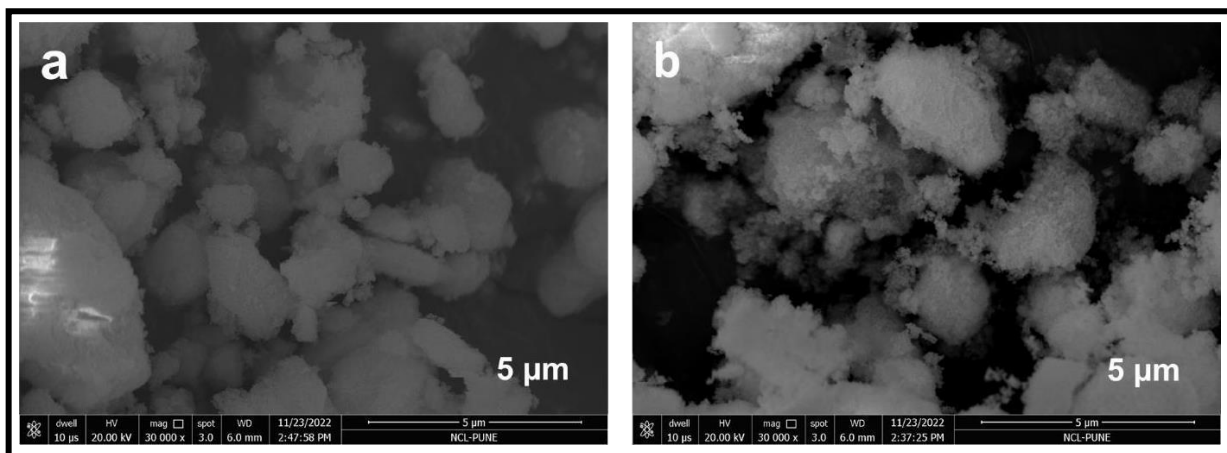


Figure 3.4 SEM images of (a)  $\text{Ce}_{0.75}\text{Zr}_{0.25}\text{O}_2$  calcined at  $1000^\circ\text{C}$ ; (b)  $1\%\text{Pd}/\text{Ce}_{0.75}\text{Zr}_{0.25}\text{O}_2$  calcined at  $500^\circ\text{C}$

Table 3.2 Elemental analysis of catalysts by EDAX

S.N.	Catalyst	Elemental composition (%)			
		Pd	Ce	Zr	O
1	$\text{Ce}_{0.75}\text{Zr}_{0.25}\text{O}_2$ ( $600^\circ\text{C}$ )	0.00	60.72	14.45	24.82
2	$\text{Ce}_{0.75}\text{Zr}_{0.25}\text{O}_2$ ( $1000^\circ\text{C}$ )	0.00	59.29	17.59	22.98
3	$1\%\text{Pd}/\text{Ce}_{0.75}\text{Zr}_{0.25}\text{O}_2$ ( $500^\circ\text{C}$ )	1.06	59.13	13.29	26.52

### 3.1.5 TEM Analysis

The TEM investigation was used to determine the palladium and ceria-zirconia particle sizes for all of the synthesized catalysts, as shown in Figures 3.5 to 3.7. The d-spacing values allowed us to identify the palladium, ceria and zirconia particles. In the all-figures d-spacing values are shown. For a catalyst containing  $\text{Ce}_{0.75}\text{Zr}_{0.25}\text{O}_2$  ( $600^\circ\text{C}$ ), the majority of the particles were found to be 23–24 nm in size, with the particle size distribution ranging from 10–35 nm with d-spacing values of ceria (111), zirconia (220) to be 0.27 nm, 0.16 nm respectively (Figure 3.5). Palladium nanoparticles with d-spacing of 0.23 nm, which corresponds to the (111) plane of the Pd metal and particle size in the range 1.5–1.95 nm, were visible in the microscopic analysis (Figure 3.7).

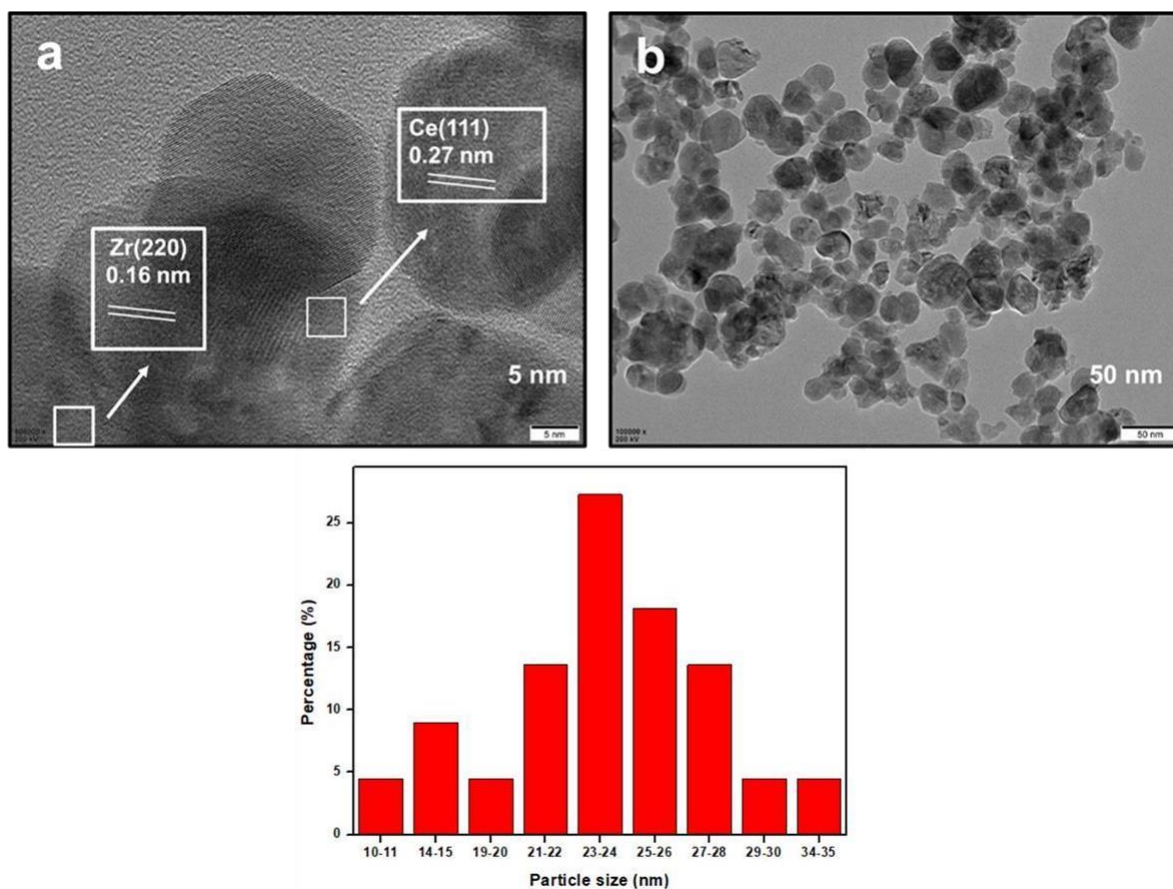


Figure 3.5 TEM images of  $\text{Ce}_{0.75}\text{Zr}_{0.25}\text{O}_2$  calcined at  $600^\circ\text{C}$

Generally, ceria has most stable cubic (111) plane while zirconia has temperature dependent planes, at low temperature it shows monoclinic and high temperature it transforms to a tetragonal phase. Therefore, zirconia shows (220) plane in catalyst  $\text{Ce}_{0.75}\text{Zr}_{0.25}\text{O}_2$  calcined at low temperature ( $600^\circ\text{C}$ ) and (200) plane in catalyst  $\text{Ce}_{0.75}\text{Zr}_{0.25}\text{O}_2$  calcined at high temperature ( $1000^\circ\text{C}$ ). From the image of the catalyst calcined at high temperature, it is understood that the particles agglomerate in high temperature, which increases the particle size. The size of most of the particles of the catalyst were in the range of 40-45 nm and the particle size distribution were in the range of 20-55 nm (Figure 3.6).

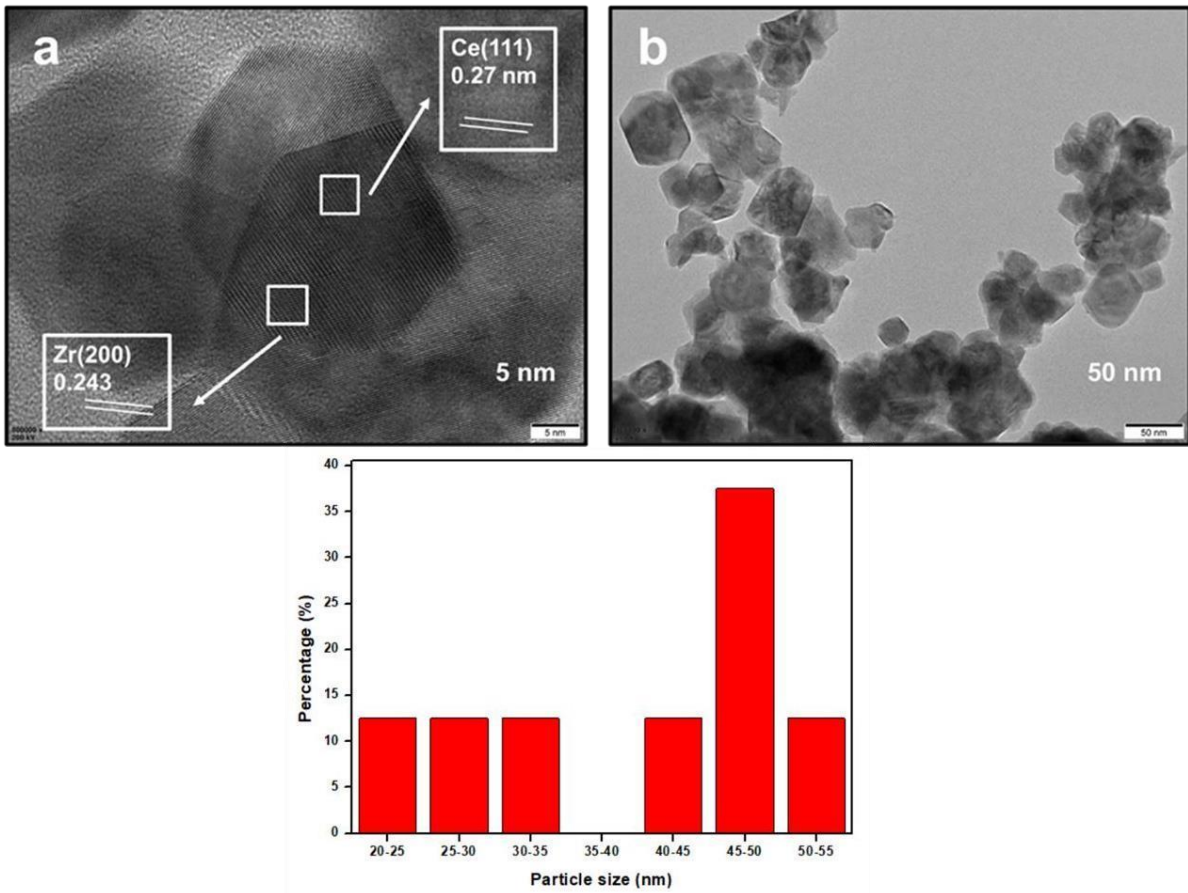


Figure 3.6 TEM images of  $\text{Ce}_{0.75}\text{Zr}_{0.25}\text{O}_2$  calcined at  $1000^\circ\text{C}$

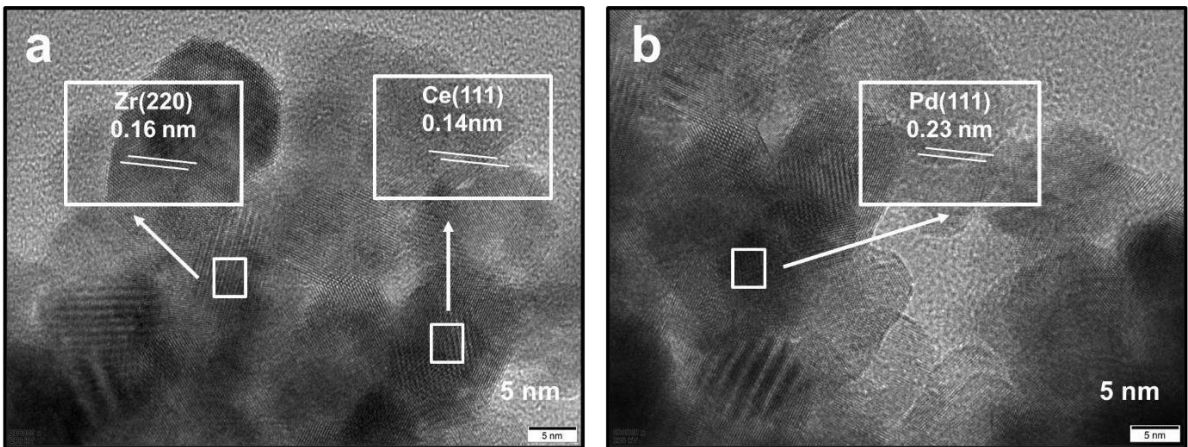


Figure 3.7 TEM images of 1% Pd/ $\text{Ce}_{0.75}\text{Zr}_{0.25}\text{O}_2$  calcined at  $500^\circ\text{C}$

### 3.1.6 X-ray photoelectron spectroscopy analysis

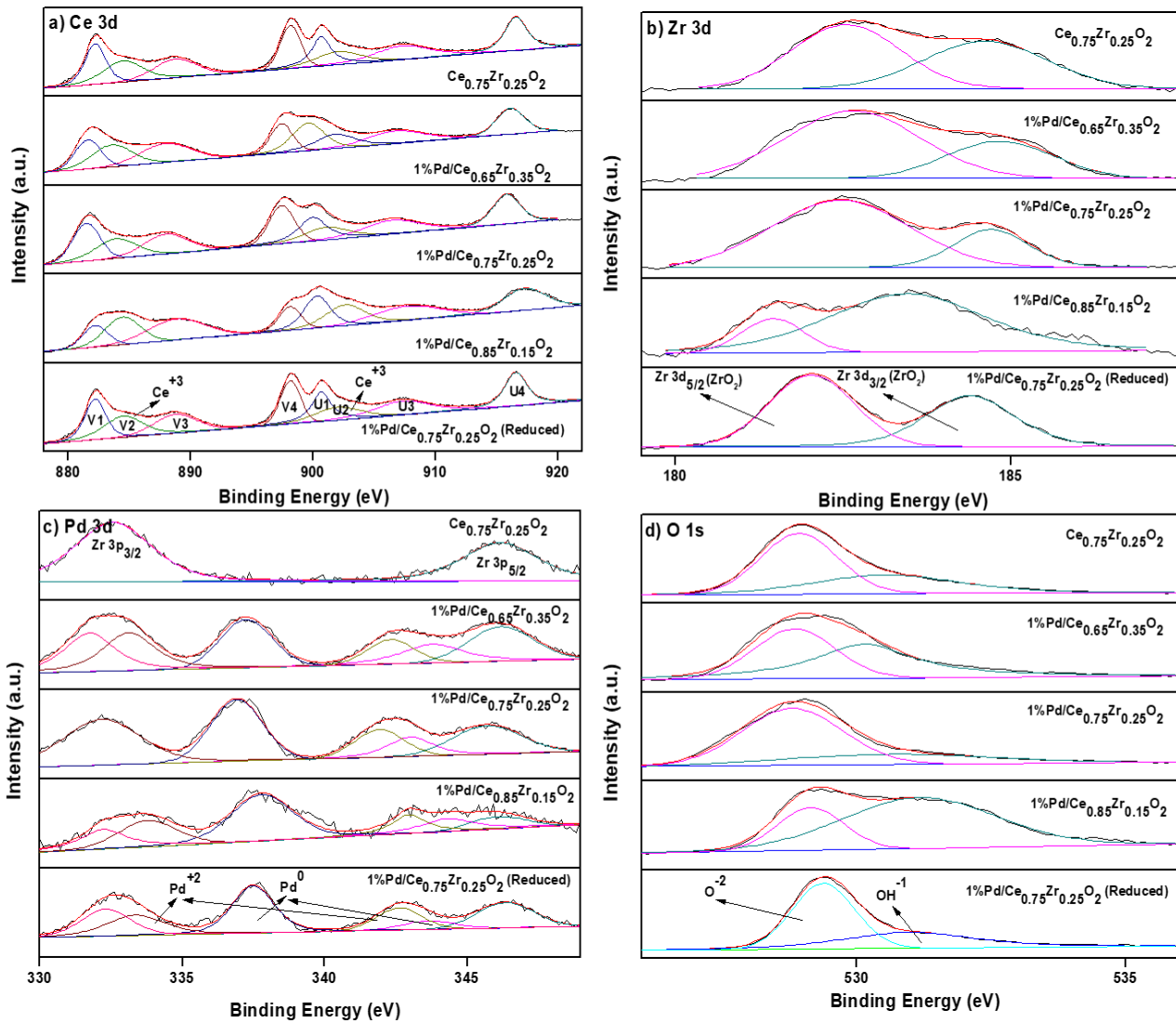


Figure 3.8 a) Ce 3d, b) Zr 3d, c) Pd 3d, and d) O 1s XPS spectra

To verify the variations between the oxidation states of prepared catalyst composition and reduced catalyst, the XPS analysis was conducted.

The Ce 3d XPS spectra for each sample are displayed in Figure 3.8(a). The Ce 3d<sub>5/2</sub> and Ce 3d<sub>3/2</sub> ionisations make up the Ce 3d peak separations. The Ce 3d<sub>5/2</sub> ionisation is represented in the image by the peaks labelled V1, V2, V3, and V4, while the Ce 3d<sub>3/2</sub> ionisation is represented by the peaks U1, U2, U3, and U4. [20,29] The Ce<sup>4+</sup> ions are said to be responsible for the peaks V1, V3, V4, U1, U3, and U4, while the Ce<sup>+3</sup> ions are stated to be responsible for the peaks V2 and U2 [30].

The V and U peak areas were used to determine the concentrations of Ce<sup>+3</sup> ions as follows:

$$[\text{Ce}^{+3}] = (\text{V2} + \text{U2}) / (\text{V1} + \text{V2} + \text{V3} + \text{V4} + \text{U1} + \text{U2} + \text{U3} + \text{U4})$$

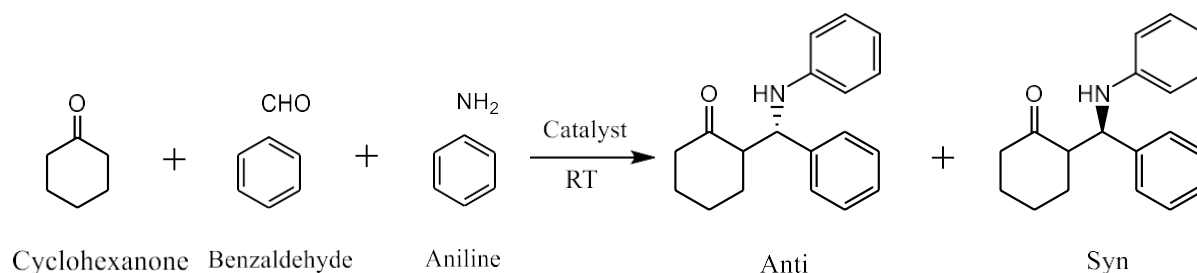
Concentration of  $\text{Ce}^{+3}$  ions written along to the samples are  $\text{Ce}_{0.75}\text{Zr}_{0.25}\text{O}_2$  (21.14%), 1%Pd/ $\text{Ce}_{0.65}\text{Zr}_{0.35}\text{O}_2$  (13.16), 1%Pd/ $\text{Ce}_{0.75}\text{Zr}_{0.25}\text{O}_2$  (22%), 1%Pd/ $\text{Ce}_{0.85}\text{Zr}_{0.15}\text{O}_2$  (26%), and 1%Pd/ $\text{Ce}_{0.75}\text{Zr}_{0.25}\text{O}_2$  (reduced) (23.30%). This shows that most of the cerium is present in the form of  $\text{CeO}_2$  ( $\text{Ce}^{+4}$ ) in all the samples.

The dissociation of  $\text{H}_2\text{O}$  caused by the presence of  $\text{Ce}^{+3}$  ions in aqueous environments produces hydroxyl (OH) groups on the surface. [31, 32] These OH groups serve as reactive sites for the adsorption of other compounds, in particular [33]. O 1s XPS analysis was used to identify the concentrations of surface OH and  $\text{O}^{-2}$  groups [Fig. 3.8(d)]; the two peaks seen in the XPS spectra were assigned to lattice oxygen  $\text{O}^{-2}$  and surface OH. [34, 35] the Zr 3d spectrum (Fig. 3.8(b)) shows Zr  $3d_{5/2}$  and Zr  $3d_{3/2}$  emissions of  $\text{Zr}^{+4}$  ion and their binding energy in all samples are near & equal to 181.84 eV and 184.30 eV. [36]

Figure 3.8(c) shows the XPS spectra of the Pd 3d. The peaks of Zr 3p occur in this range as shown in the image. The relative binding energy of  $3p_{3/2}$  and  $3p_{1/2}$  is 331.90, 346 eV. Palladium in the complex is showing 0 and +2 oxidation states as determined by its binding energy. The binding energy related to  $\text{Pd}^0$  is approx. 337, 343.85 eV while the binding energy related to  $\text{Pd}^{+2}$  is approx. 333, 342.60 eV [37].

### 3.2 Catalytic activity for Mannich reaction

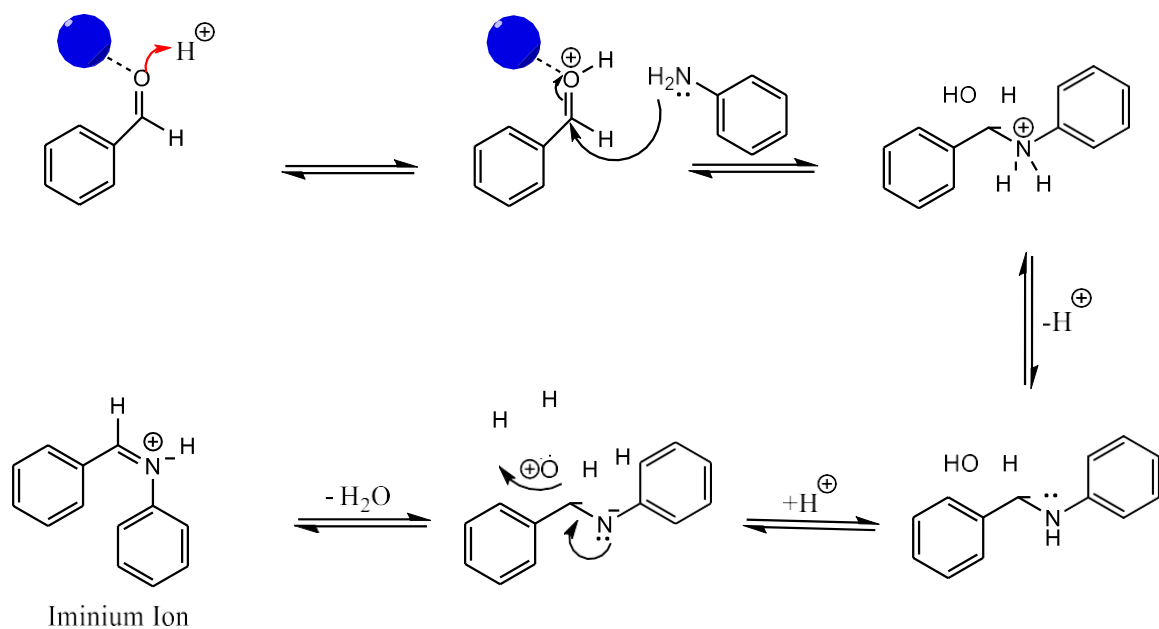
The Mannich (three component) reaction was carried out with  $\text{Ce}_{0.75}\text{Zr}_{0.25}\text{O}_2$  and 1% Pd/ $\text{Ce}_{0.75}\text{Zr}_{0.25}\text{O}_2$  catalysts, which was carried out according to the scheme as shown (3.1) show below. To see the effect of time in this reaction, we conducted the reaction in different time.



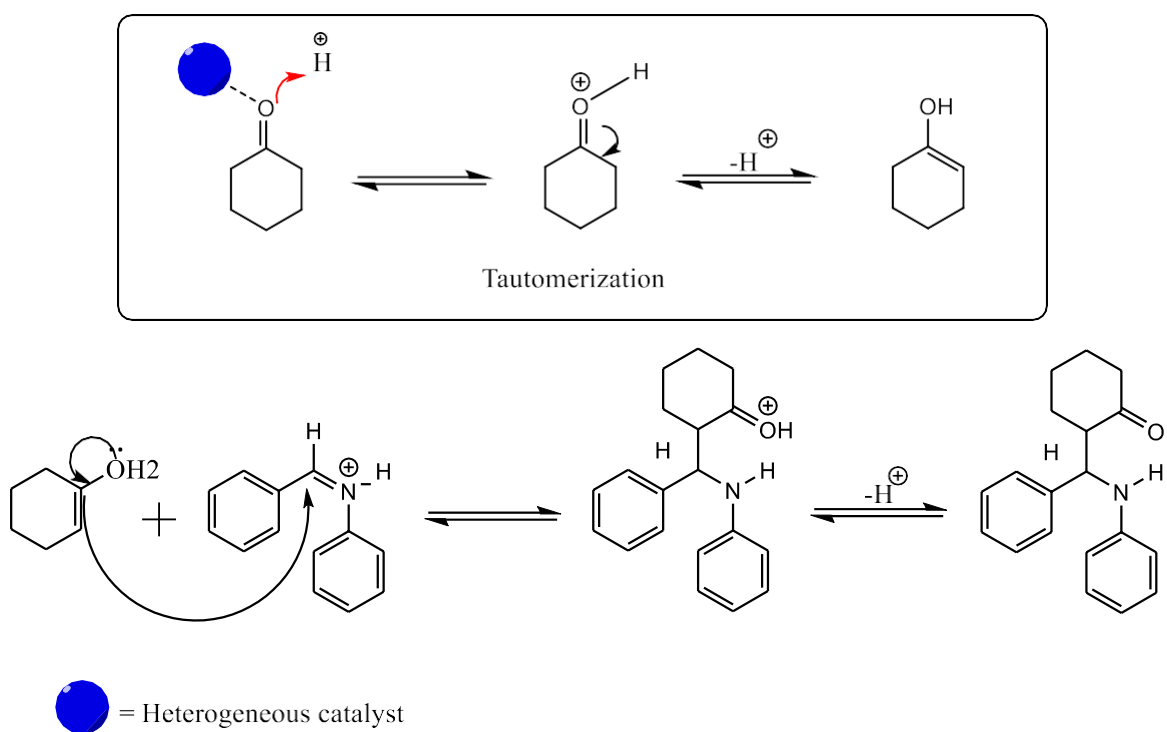
Scheme 3.1 Mannich reaction with reactant cyclohexanone, benzaldehyde and aniline

When the reactions were analysed, it was found that there was no change in the yield with time. The main reason for this is the acid sites of the catalysts [38], there is not that much acid sites in the catalysts to get this reaction done. This is the reason why this reaction shows very low (<10%) yield.

### Step First- Formation Of Iminium Ion



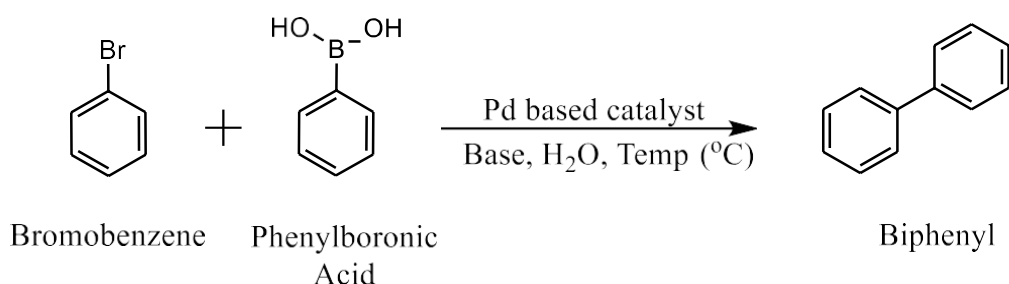
### Step Second- Formation Of $\beta$ -amino carbonyl compound



Scheme 3.2 possible mechanism for Mannich (three component) reaction

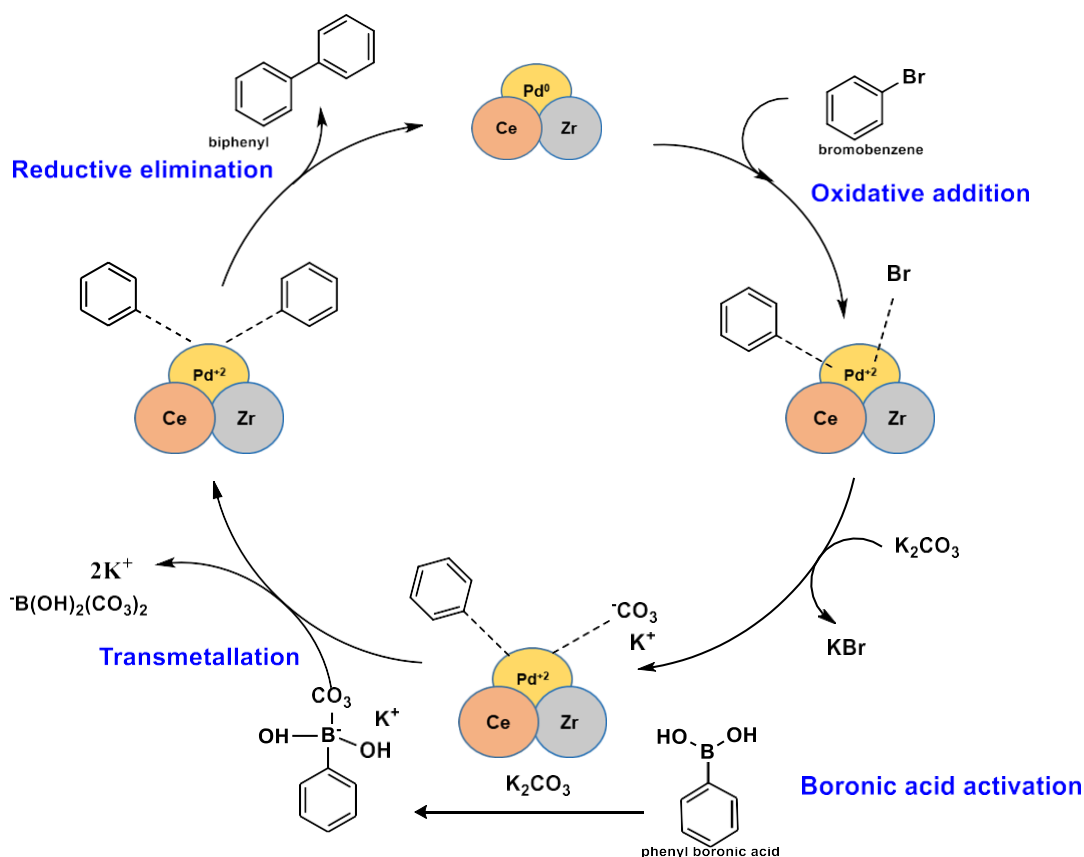
### 3.3 Catalytic activity for Suzuki coupling reaction

The reaction was carried out according to the scheme 3.3 show below.



Scheme 3.3 Suzuki coupling reaction with bromobenzene and phenylboronic acid

In Suzuki coupling reaction the reactants change to product in the presence of Pd based catalysts. Whose complete mechanism is shown in scheme 3.4.



Scheme 3.4 Mechanism of Suzuki coupling reaction catalysed by Pd/Ceria-Zirconia

In this reaction, we have studied some parameters whose details are as follows.

### 3.3.1 Base effect on Suzuki coupling reaction

To see the effect of base in the reaction, different bases were used and the yield that shown in table 3.3. Analyzing all the reactions, it is found that NaOH promotes product formation the most. Also, we can say that Suzuki coupling reaction is more favored by strong base as compare to weak base.

Table 3.3 Effect of bases in Suzuki coupling reaction

S.N.	Base	Yield (%)
1	NaOH	69.25
2	Na <sub>2</sub> CO <sub>3</sub>	13.26
3	KOH	69.14
4	K <sub>2</sub> CO <sub>3</sub>	64.56
5	CaCO <sub>3</sub>	5.75
6	Ca(OH) <sub>2</sub>	5.51
7	Ba(OH) <sub>2</sub>	18.07

Reaction condition – bromobenzene (1 gm), phenylboronic acid (0.932 gm), different base, water (2 ml) and 5 wt% 1% Pd/Ce<sub>0.75</sub>Zr<sub>0.25</sub>O<sub>2</sub> catalyst at 100°C for 3 h

### 3.3.2 Time profile study of Suzuki coupling reaction

To understand the effect of reaction time, reactions were carried out for different times. Whose details are given in table 3.4. Looking at these data, it is clear that as the reaction time is increasing, the yield is also increasing.

Table 3.4 Time profile study of Suzuki coupling reaction

S.N.	Time (hour)	Yield (%)
1	3	64.56
2	4	69.25
3	5	76.73
4	6	81.98
5	7	85.55
6	8	90.13
7	11	92.02

Reaction condition – bromobenzene (1 gm), phenylboronic acid (0.932 gm),  $K_2CO_3$ , water (2 ml) and 5 wt% 1% Pd/Ce<sub>0.75</sub>Zr<sub>0.25</sub>O<sub>2</sub> catalyst at 100°C for different time.

### 3.3.3 Effect of catalyst composition on Suzuki coupling reaction

Different compositions of palladium and ceria-zirconia were synthesized and reactions were carried out with them to reveal the effect of catalyst composition. The data of all these reactions are shown in table 3.5.

Table 3.5 Effect of catalyst composition on Suzuki reaction

S.N.	Catalyst composition	Yield (%)
1	1% Pd/Ce <sub>0.65</sub> Zr <sub>0.35</sub> O <sub>2</sub>	67.24
2	1% Pd/Ce <sub>0.75</sub> Zr <sub>0.25</sub> O <sub>2</sub>	64.56
3	1% Pd/Ce <sub>0.85</sub> Zr <sub>0.15</sub> O <sub>2</sub>	36.14

Reaction conditions – bromobenzene (1 gm), phenylboronic acid (0.932 gm),  $K_2CO_3$ , water (2 ml) and 5 wt% different catalyst composition at 100°C for 3 h

### 3.3.4 Effect of Temperature on Suzuki coupling reaction

The effect of temperature on Suzuki coupling reaction was studied and results are shown in Table 3.6. In this case, the reaction was carried out at three different temperatures i.e., RT, 70°C and 100°C.

Table 3.6 Effect of temperature on Suzuki reaction

S.N.	Temperature (°C)	Yield (%)
1	32 (RT)	12.04
2	70	28.84
3	100	67.24

Reaction condition – bromobenzene (1 gm), phenylboronic acid (0.932 gm),  $K_2CO_3$ , water (2 ml) and 5 wt% 1% Pd/Ce<sub>0.65</sub>Zr<sub>0.35</sub>O<sub>2</sub> catalyst at different temperature for 3 h

### 3.3.5 Effect of Catalyst loading on Suzuki coupling reaction

The amount of catalyst plays a very important role in any catalytic reaction. Therefore, different weight percentage (wt%) catalyst reactions were carried out, from which the effect of catalyst loading could be understood. All of these reaction's data are shown in the table 3.7 below.

Table 3.7 Effect of catalyst loading on Suzuki reaction

S.N.	Catalyst loading (wt%)	Yield (%)
1	2.5	35.18
2	5	67.24
3	10	63.12

Reaction condition – bromobenzene (1 gm), phenylboronic acid (0.932 gm),  $K_2CO_3$ , water (2 ml) and different wt% 1% Pd/Ce<sub>0.65</sub>Zr<sub>0.35</sub>O<sub>2</sub> catalyst at 100°C for 3 h

## 4. Conclusion

The ceria-zirconia mixed oxide is prepared by the hydrothermal method and 1% palladium is loaded onto the composition by the impregnation method. The mixed support was calcined at different temperatures. Detailed characterization of the catalysts helped understand the nature and characteristics of the prepared materials. The high crystallinity of the compositions at high calcination temperature was confirmed by P-XRD. Similarly BET analysis revealed decrease in surface area with increase in the calcination temperature. From SEM and TEM, it was found that cerium, zirconium, palladium and oxygen are present in the compositions and their particle size is in nanometer range. The oxidation state of the cerium (Ce<sup>+3</sup>, Ce<sup>+4</sup>), zirconium (Zr<sup>+4</sup>) and palladium (Pd<sup>0</sup>, Pd<sup>+2</sup>) was confirmed by XPS analysis. Also, the concentration Ce<sup>+3</sup> of showed that cerium in the compositions mostly existed in Ce<sup>+3</sup> oxidation state.

The 1%Pd/Ce<sub>0.65</sub>Zr<sub>0.35</sub>O<sub>2</sub>, catalyst has shown promising activity for Suzuki coupling reaction of bromobenzene and phenyl boronic acid and the effect of different reaction on product yield was studied. The results revealed that strong bases favor this reaction and increases the product yield by increasing the reaction time.

## References

1. Silberberg, Martin Stuart, et al. *Chemistry: The molecular nature of matter and change*. Vol. 4. New York: McGraw-Hill, 2006
2. van Leeuwen, Piet WNM. "Introduction: What it is all about." *Homogeneous Catalysis: Understanding the Art* (2004): 1-28.
3. E. Roduner, *Chem. Soc. Rev.*, 2014, 43, 8226-8239.
4. American Chemical Society Report, *Technology Vision 2020: The Chemical Industry*, December 1996.
5. *Catalysis: From Principles to Applications*, First Edition. Edited by M. Beller, A. Renken, and R. van Santen 2012 Wiley-VCH Verlag GmbH & Co. KGaA.
6. R. A. Van Santen, M. Neurock, *Molecular heterogeneous catalysis: a conceptual*

7. S. Vaclav, *Nature*, 1999, 400, 415.
8. Leach, E. Bruce., 1983, *Industrial Catalysis: Chemistry applied to your life-style and environment*, In *Applied industrial catalysis*, vol 1, New York, Academic press, Inc.
9. G. Ertl (*Catalysis: Science and Technology*, 1. R. Anderson and M. Boudart, Eds., vol. 4, Springer-Verlag, Berlin, 1983, p. 245.
10. Adlercreutz, Patrick; Straathof, Adrie J., *J. Applied Biocatalysis* (2nd ed.), Faber, Kurt (2011). *Biotransformations in Organic Chemistry* (6th ed.). Springer.
11. Rothenberg, Gadi (2008). *Catalysis: Concepts and green application*.
12. (a) A. Bhangale, K. Santanu, E. William; M. F. Kathleen; M. G. Charles; A. G. Richard; L. B. Kathryn *JACS*, 2010, 133, 6006–6011; (b) A. Bhangale, L. B. Kathryn, A. G. Richard, *Macromol.*, 2012, 45, 7000-7008.
13. G. A. Somorjai, *Introduction to Surface Chemistry and Catalysis*, John Wiley, New York, 1994, p. 667.
14. R. L. Burwell, G. L. Haller, K. C. Taylor, J. F. Read, *Adv. Synth. Catal.*, 1969, 29, 1.
15. (a) G. Ertl, H. Knözinger, J. Weitkamp (eds.): *Handbook of Heterogeneous Catalysis*, Vol. 1, Wiley-VCH, Weinheim 1997, p. 216; (b) G. C. Bond in G. Ertl, H. Knözinger, J. Weitkamp (eds.): *Handbook of Heterogeneous Catalysis*, Vol. 2, Wiley-VCH, Weinheim 1997, p. 752.
16. C. J. Pan, M. C. Tsai, W. N. Su, J. Rick, N. G. Akalework, A. K. Agegnehu, S. Y. Cheng, B. J. Hwang, *Engineers*, 2017, 74, 154-186.
17. B. D. Adams, A. Chen, *Mater. Today*, 2011, 14, 282-289.
18. (a) H. R., Crabtree; "Application to Organic Synthesis" *The Organometallic Chemistry of the Transition Metals*. John Wiley and Sons, (2009) pp 392. 12. E., Christine (b) G. K., Prasad; "The Art of Meeting Palladium Specifications in Active Pharmaceutical Ingredients Produced by Pd-Catalyzed Reactions" *Advanced Synthesis & Catalysis*, (2004), vol 8, pp 889–900.
19. E. Gbenedio, Z. Wu, I. Hatim, B. F. K. Kingsbury, K. Li, *Catal. Today*, 2010, 156, 93- 99.
20. L. Rodríguez, D. Romero, D. Rodríguez, J. Sánchez, F. Domínguez, G. Arteaga, *Appl. Catal. A*, 2010, 373, 66-70.
21. C. R. Lederhos, M. J. Maccarrone, J. M. Badano, G. Torres, F. Coloma-Pascual, J. C. Yori, M. E. Quiroga, *Appl. Catal. A*, 2011, 396, 170-176.
22. Y. Bi, H. Xu, W. Li, A. Goldbach, *Int. J. Hydrogen Energy*, 2009, 34, 2965-2971.
23. L. S. F. Feio, C. E. Hori, S. Damyanova, F. B. Noronha, W. H. Cassinelli, C. M. P. Marques, J. M. C. Bueno, *Appl. Catal. A*, 2007, 316, 107-116.
24. J. A. Moulijn, P. W. N. M. van Leeuwen, R. A. van Santen, *Stud. Surf. Sci. Catal.*, Elsevier, 1993, 79, 419.
25. E. Abdellatif, S. E. Kazzouli, M. Bousmina, *J. Nanosci. Nanotechnol.*, 2014, 14, 2012- 202.
26. T. Punniyamurthy, S. Velusamy, J. Iqbal, *Chem. Rev.*, 2005, 105, 2329-2364.
27. Maddila, Surya Narayana, et al. *Research on Chemical Intermediates* 43.8 (2017): 4313-4325.
28. Farahmandjou, M., M. Zarinkamar, and T. P. Firoozabadi. *Revista mexicana de física* 62.5 (2016): 496-499.
29. Patel, Sweetu B., et al. *RSC advances* 7.48 (2017): 30397-30410.
30. J. Shyu, W. Weber, and H. Gandhi: Surface characterization of alumina-supported ceria. *J. Phys. Chem.* 92, 4964 (1988).

31. S.D. Senanayake, D. Stacchiola, J. Evans, M. Estrella, L. Barrio, M. Pérez, J. Hrbek, and J.A. Rodriguez: Probing the reaction intermediates for the water–gas shift over inverse CeOx/Au(111) catalysts. *J. Catal.* 271, 392 (2010).
32. Zhang, Y. Yu, M.E. Grass, C. Dejoie, W. Ding, K. Gaskell, N. Jabeen, Y.P. Hong, A. Shavorskiy, and H. Bluhm: Mechanistic studies of water electrolysis and hydrogen electro-oxidation on high temperature ceria-based solid oxide electrochemical cells. *J. Am. Chem. Soc.* 135, 11572 (2013).
33. C. Armistead, A. Tyler, F. Hambleton, S. Mitchell, and J.A. Hockey: Surface hydroxylation of silica. *J. Phys. Chem.* 73, 3947 (1969).
34. B. Erdem, R.A. Hunsicker, G.W. Simmons, E.D. Sudol, V.L. Dimonie, and M.S. El-Aasser: XPS and FTIR surface characterization of TiO<sub>2</sub> particles used in polymer encapsulation. *Langmuir* 17, 2664 (2001).
35. J. Van den Brand, W. Sloof, H. Terryn, and J. De Wit: Correlation between hydroxyl fraction and O/Al atomic ratio as determined from XPS spectra of aluminium oxide layers. *Surf. Interface Anal.* 36, 81 (2004).
36. Bumajdad, Ali, et al. "Controlled synthesis of ZrO<sub>2</sub> nanoparticles with tailored size, morphology and crystal phases via organic/inorganic hybrid films." *Scientific reports* 8.1 (2018): 3695.
37. Wang, Tong, et al. "Enhanced catalytic activity over palladium supported on ZrO<sub>2</sub>@ C with NaOH-assisted reduction for decomposition of formic acid." *RSC advances* 9.6 (2019): 3359-3366.
38. Reddy, Benjaram M., et al. *Journal of Molecular Catalysis A: Chemical* 244.1-2 (2006): 1-7.

